CrossMark

**ORIGINAL ARTICLE**

# Existence of traversable wormholes in the spherical stellar systems

**A. Övgün[1] · M. Halilsoy[1]**

**Abstract** Potentiality of the presence of traversable wormholes in the outer/inner regions of the halos of galaxies, situated on the Navarro-Frenk-White (NFW) density profile and Universal Rotation Curve (URC) dark matter models have been investigated recently (Rahaman et al. in Eur. Phys. J. C 74:2750, 2014a; Rahaman et al. in Ann. Phys. 350:561–567, 2014b; Kuhfittig in Eur. Phys. J. C 74:2818, 2014a; Kuhfittig in Found. Phys. 7:111–119, 2014b; Kuhfittig in Int. J. Mod. Phys. D 24(03):1550023, 2015; Rahaman et al. in Astrophys. Space Sci. 361(1):37, 2016a; Rahaman et al. in Astrophys. Space Sci. 361(3):90, 2016b). Since this covers our own galaxy also as a possible home for traversable wormholes it prompts us to further the subject by considering alternative density distributions. From this token herein we make use of the Einasto model (Einasto in Tr. Inst. Astrofiz. Alma-Ata 5:87, 1965; Einasto and Haud in Galaxy Astron. Astrophys. 223:89, 1989; Merritt et al. in Astron. J. 132:6, 2006) to describe the density profiles for the same purpose. Our choice for the latter is based on the fact that theoretical dark matter halos produced in computer simulations are best described by such a profile. For technical reasons we trim the number of parameters in the Einasto profile to a possible minimum. Based on such a model it is shown that traversable wormholes in the outer regions of spiral galaxies are possible while the inner part regions prohibit such formations.

**Keywords** Wormholes · Milky Way · Spherical stellar systems · Galaxies · Halos · Dark matter

✉ A. Övgün
ali.ovgun@emu.edu.tr

[1] Physics Department, Eastern Mediterranean University, Northern Cyprus, Mersin 10, Famagusta, Turkey

## 1 Introduction

Although Flamm's work on the wormhole physics dates back to 1916, in connection with the newly found Schwarzschild solution (Flamm 1916), wormhole solutions were firstly considered from physics standpoint by Einstein and Rosen (ER) in 1935, which is known today as Einstein-Rosen bridge connecting two identical space-times (Einstein and Rosen 1935). Then in 1955 Wheeler used "geons" (self-gravitating bundles of electromagnetic fields) by giving the first diagram of a doubly-connected-space (Wheeler 1955). Wheeler added the term "wormhole" to the physics literature, however he defined it at the quantum scale. After that, first traversable wormhole was proposed by Morris-Thorne in 1988 (Morris and Thorne 1988). Then Morris, Thorne, and Yurtsever investigated the requirements of the energy condition for wormholes (Morris et al. 1988). After while, Visser constructed a technical way to make thin-shell wormholes which thoroughly surveyed the research landscape as of 1988 (Poisson and Visser 1955; Visser 1989a, 1989b; Visser et al. 2003). After this, there are many papers written to support this idea (Halilsoy et al. 2014; Mazharimousavi and Halilsoy 2015a, 2015b; Ovgun and Sakalli 2015).

In 1933 F. Zwicky, was the first astronomer to propose the existence of the dark matter (DM) after that he observed the motions of the galaxies in the Coma Cluster, a galaxy cluster roughly 320 million light-years away and nearly 2 light-years across, and found that it moved too rapidly (Zwicky 1933). He noted that its speed of revolution, which depends on the weight and position of the objects inside, implied the cluster had much more mass than he could see. He decided there must be a hidden ingredient, known as dark matter, that caused the motions of these galaxies to be so large. In 1978, American astronomer

Vera Rubin looked at individual galaxies and she realized that the outer stars were spinning as quickly as the interior stars, and sometimes faster (Vera and Kent 1970). It is concluded that the galaxies must be surrounded by a halo of matter which is not seen. Theorists have postulated many candidates for what DM might be. But the most widely accepted hypothesis is the weakly interacting massive particles (WIMPs), a particle that interacts with gravity but not light, hence its invisibility to us (Cui 2015). Neither WIMPs nor any other particle that could successfully explain DM exist in the standard model of particle physics, the theoretical framework that has successfully predicted nearly all the phenomena in the universe. Thus, the identity of the DM particle remains one of the outstanding mysteries in particle physics and cosmology. According to the latest results from the Planck satellite (Ade et al. 2014), a mere 26.8 % DM percent of the universe which plays a central role in modeling of cosmic structure, galaxy formation and evolution and on explanations of the anisotropies observed in the cosmic microwave background (CMB), 4.9 % is made of ordinary matter which is matter composed of atoms or their constituents and 68.3 % is dark energy (DE) that tends to accelerate the expansion of the universe (Garrett et al. 2011; Cline 2016; Gaskins 2016). Certain types of DM can actually help the formation of wormholes. For example, dissipative DM in which DM particles forming galactic halos are presumed to have dissipative self-interactions can aid the formation of black holes by dissipative collapse, and subsequent to wormholes. Now, in this types of models one can consider either DM collapsed to a disk, or a quasi-isothermal profile (Fan et al. 2013a, 2013b; Foot and Vagnozzi 2015; Myrzakulov et al. 2015; Kirillov and Savelova 2015).

Recently, Rahaman et al. have used both the NFW (Navarro et al. 1996; Rahaman et al. 2016a, 2016b)

$$\rho(r) = \frac{\rho_s}{\frac{r}{r_s}(1 + \frac{r}{r_s})^2}, \tag{1}$$

and URC DM density profiles (Castignani et al. 2012)

$$\rho(r) = \frac{\rho_0 r_0^3}{(r + r_0)(r^2 + r_0^2)} \tag{2}$$

where $\rho_0$, $\rho_s$, $r_0$ and $r_s$ are all constants, to show the potentiality of the presence of traversable wormholes in the outer and the inner part, respectively, of the halo.

In this paper, following similar line of thought, we study the Einasto model (Einasto 1965; Einasto and Haud 1989; Merritt et al. 2006) which is the special function that arranges the finest total fit to the halo density profiles. It tells how the density $\rho$ of a spherical stellar system changes with distance $r$ from its center (Hjorth et al. 2015): This is expressed by the density profile

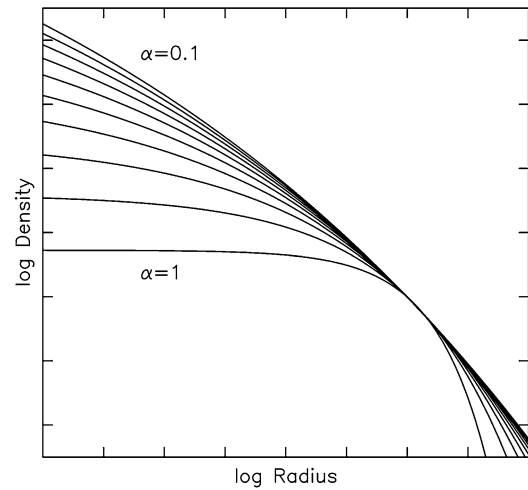$$\rho(r) \propto e^{-Ar^\alpha} \tag{3}$$

with constants $A$ and $\alpha$.

**Fig. 1** Einasto profile in log-log plot (the parameter $\alpha$ controls the degree of curvature of the profile) from Eq. (3)
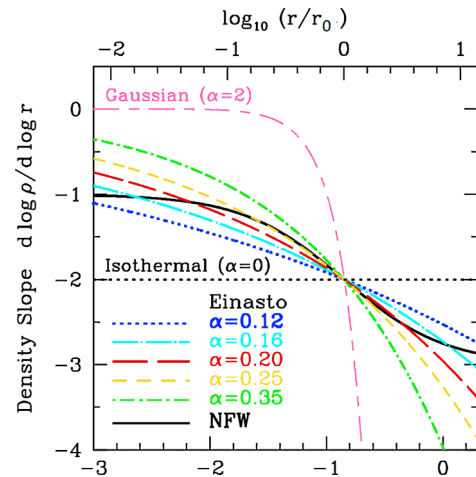


**Fig. 2** Density profiles of Einasto and NFW, density slope ($d \log \rho / d \log r$) (Dutton and Maccio 2014)

The bounded parameter $\alpha$ which is called Einasto index, adjusts the degree of curvature of the profile (Dhar and Williams 2010; Retana-Montenegro et al. 2012)

$$\rho(r) = \rho_0 \exp\left[-\frac{2}{\alpha}\left(\left(\frac{r}{r_0}\right)^\alpha - 1\right)\right], \tag{4}$$

simply named as the Einasto model in the present paper which is plotted in Fig. 1. For the Milky Way galaxy, we have $r_0 = 9.11$ kpc and $\rho_0 = 5 \times 10^{-24}(r_0/8.6 \text{ kpc})^{-1}$ g cm$^{-3}$ (Maccio et al. 2012; Castignani et al. 2012).

The slopes of the NFW profile has the range from the inner/outer ($r \to 0/r \to \infty$) are depicted in Figs. 2 and 3 below. On the other hand, the values are different for the Einasto profile which are included as limiting cases of isothermal and Gaussian, ($\alpha = 0$, $\alpha = 2$, respectively). The difference between the Einasto and NFW profiles appears at small and large radial distances. After all, on scales of
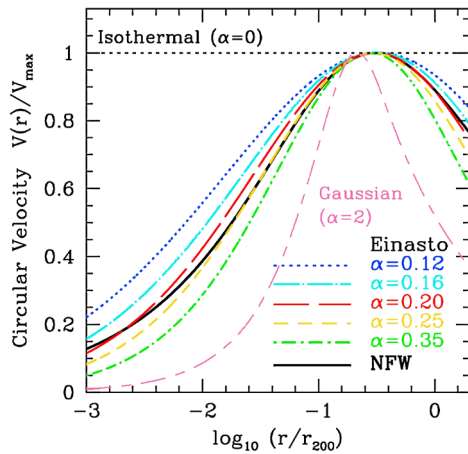
**Fig. 3** Comparison of NFW (*solid black lines*) and Einasto (*colored lines*) profiles. In this example the halo concentration $c_{200} = 7.1$ (Dutton and Maccio 2014)

concern for gas or stellar dynamics and strong gravitational lensing the Einasto profile with $\alpha = 0.25$ is very akin to the NFW profile, and on scales of concern for weak gravitational lensing the Einasto profile with $\alpha = 0.2$ is quite similar to the NFW profile. Galaxy mass halos typically have $\alpha = 0.16$ as referred in Figs. 2 and 3 (Dutton and Maccio 2014).

Einasto's model has been used in the description of many systems, such as galaxies, and halos. It is used to show the DM profiles of simulated halos as well as the NFW profile (Bernal and Palomares-Ruiz 2012; Salvador-Sole et al. 2012; Dhar and Williams 2010). The Einasto profile has a finite (zero) central slope, in contrast to the NFW profile which has a divergent (infinite) central density. Due to the restricted resolution of N-body simulations, it is unclear yet which model description fit well to the central densities of simulated DM halo. The observations of both the Milky Way and some galaxies may be compatible with the NFW profile for the DM halo (Narikawa and Yamamoto 2012; Vera-Ciro et al. 2013; Iocco et al. 2015; Umetsu et al. 2016; Lovell et al. 2014). There are also self-interacting dark matter (SIDM) simulations and baryon feedback simulations (Rocha et al. 2013; Duffy et al. 2010; Chan et al. 2015). The SIDM is attractive because it offers a means to lower the central densities of galaxies without destroying the successes of CDM on large scales. Cosmological simulations that contain only CDM indicate that DM haloes should be cuspy and with (high) concentrations that correlate with the collapse time of the halo. One possible answer is feedback in which the expulsion of gas from galaxies can result in lower DM densities compared to dissipationless simulations, and thus bring CDM models in line with observations (Rocha et al. 2013; Vogelsberger et al. 2012). Furthermore baryon feedback has most significant effects on the inner density profiles which are typically shallower than isothermal and

the halo concentrations tend to be lower than in the absence of baryons. For instance the strong feedback models reduce the baryon fraction in galaxies by a factor of 3 relative to the case with no feedback (Chan et al. 2015).

The DM profile of smaller galaxies tend to have flatter distributions of DM in the central region, known as the cuspy halo problem (Pato and Iocco 2015; Pato et al. 2015). Our purpose in this paper is to search for possible traversable wormholes in a spiral galaxy specified by the Einasto density profile. Wormholes are solutions to Einstein's equations that connect different universes or tunnels through different parts of the same universe. Our primary aim is to consider the Milky Way galaxy as a test bed for this venture. To this end we choose the parameter $r_0$ of Milky Way to coincide with the throat of the traversable wormhole whereas the second parameter $\alpha$ is in a restricted range. From the Einstein equations we derive the equations for the density and pressures in terms of the metric functions and their derivatives. Although our analytical functions are expressed in terms of the Whittaker functions (Abramowitz and Stegun 1972) the detailed analysis are not imperative. It suffices for us to check the null-energy condition and satisfaction of the flare-out conditions (Morris and Thorne 1988; Morris et al. 1988). The same technical handicap prevents us to investigate the stability of the resulting traversable wormhole that may exist in the Milky Way galaxy. It is observed that at the central region Einasto profile does not give a traversable wormhole solution because violation of null energy condition is not satisfied there. But in the outward region we obtain possible traversable wormholes.

The paper is organized as follows. In Sect. 2 we present the Einstein equations for wormhole space-time and we find their solutions under the Einasto DM profile. In Sect. 3 we discuss our results and conclude the paper.

## 2 Traversable wormholes under the Einasto DM profile

The spherically symmetric and static wormhole geometry which was proposed by Morris-Thorne is given by the line element (Morris and Thorne 1988)

$$ds^2 = -e^{2f(r)}dt^2 + \left(1 - \frac{b(r)}{r}\right)^{-1} dr^2$$
$$+ r^2\left(d\theta^2 + \sin^2\theta d\phi^2\right), \qquad (5)$$

where the function $b(r)$ defines the spatial shape function, and $f(r)$ stands for the redshift function. The radial coordinate $r$ ranges from $+\infty$ to $b(r_0) = r_0$ (minimum radius condition that any wormhole must satisfy). The minimum value of the $r$ is $r_0$, called the throat of the wormhole. The

proper radial distance is given by

$$l(r) = \pm \int_{r_0}^{r} \frac{dr}{\sqrt{(1 - \frac{b(r)}{r})}}. \tag{6}$$

Properties of such traversable wormholes are listed below (Morris and Thorne 1988; Morris et al. 1988);

- Spherically symmetric, static metric,
- Satisfy the Einstein field equations,
- No event horizon, i.e. $e^{f(r)} \neq 0$,
- "Throat" $r = r_0$ connects two asymptotically flat space-time regions, (for Milky Way galaxy $r_0 = 9.11$ kpc),
- The stress-energy tensor (violating the null-energy condition (NEC) with $\rho + p_r < 0$, where $\rho$ is the energy density and $p_r$ the radial pressure),
- Physically reasonable construction materials, (for Milky Way galaxy $\rho_0 = 5 \times 10^{-24} (r_0/8.6 \text{ kpc})^{-1} \text{g cm}^{-3}$),
- Bearable tidal gravitational forces,
- Satisfy the flare-out condition at the throat ($b'(r_{th}) < 1$), while $b(r) < r$ near the throat,
- Finite and reasonable crossing time,
- Stable against perturbations.

The Einstein field equation are given by

$$G_\nu^\mu = 8\pi T_\nu^\mu \tag{7}$$

where $T_\nu^\mu$ is the stress-energy tensor, $G_\nu^\mu$ is the Einstein tensor with the units in which $c = G = 1$. Field equations relate space-time curvature to matter and energy distribution. The non-zero $G_\nu^\mu$ components are

$$G_t^t = -\frac{b'}{r^2}, \tag{8}$$

$$G_r^r = \frac{-b}{r^3} + 2\left(1 - \frac{b}{r}\right)\frac{f'}{r}, \tag{9}$$

$$G_\theta^\theta = G_\phi^\phi = \left(1 - \frac{b}{r}\right)\left[f'' + + f'^2 + \frac{f'}{r}\right. \\ \left. - \left(f' + \frac{1}{r}\right)\left\{\frac{b'r - b}{2r(r-b)}\right\}\right], \tag{10}$$

in which a prime is $\frac{d}{dr}$.

It is assumed that DM is expressed in the form of general anisotropic energy-momentum tensor (Rahaman et al. 2014b; Bozorgnia et al. 2013), as follows

$$T_\nu^\mu = (\rho + p_r)u^\mu u_\nu + p_r g_\nu^\mu + (p_t - p_r)\eta^\mu \eta_\nu, \tag{11}$$

in which $u^\mu u_\mu = -\frac{1}{2}\eta^\mu \eta_\mu = -1$, and where $p_t$ is the transverse pressure, $p_r$ is the radial pressure and $\rho$ is the energy density. A possible set of $u^\mu$ and $\eta^\mu$ are given by $u^\mu = (e^{2f(r)}, 0, 0, 0)$ and $\eta^\mu = (0, 0, \frac{1}{r}, \frac{1}{r \sin \theta})$. Let us add that once we restrict ourselves entirely to a collisionless cold

DM the pressure terms should not be taken into account. Our choice implies accordingly that we aim a more general anisotropic fluid, at least for our future interest. The only non-zero components of $T_\nu^\mu$ are

$$T_t^t = -\rho, \tag{12}$$

$$T_r^r = p_r, \tag{13}$$

$$T_\theta^\theta = T_\phi^\phi = p_t. \tag{14}$$

Furthermore we need to impose some constraints in order to solve Einstein field equations. One of them is the tangential velocity, (for a justification of this condition we refer to the book by Chandrasekhar 1983 and Landau and Lifshitz 1975)

$$v^\phi = \sqrt{rf'} \tag{15}$$

which is responsible to fit the flat rotational curve for the DM (see Figs. 4 and 5). Other one is proposed by Rahaman et al. (2014b) that the observed rotational curve profile in the DM region is given by

$$v^\phi = \alpha r \exp(-k_1 r) + \beta\left[1 - \exp(-k_2 r)\right] \tag{16}$$

in which $\alpha$, $\beta$, $k_1$, and $k_2$ are constant positive parameters. It is illustrated in Fig. 6. With this choice it is guaranteed that for $r \longrightarrow \infty$ we obtain $v^\phi = \beta = $ constant which is required for flat rotation curves.

From Eqs. (15) and (16), one obtains the redshift function as follows

$$f(r) = -\frac{\alpha^2 r}{2k_1 e^{(2k_1 r)}} - \frac{\alpha^2}{4k_1^2 e^{(2k_1 r)}} - \frac{2\alpha\beta}{k_1 e^{(k_1 r)}} \\ + \frac{2\alpha\beta e^{(-k_1 r - k_2 r)}}{k_1 + k_2} + \beta^2 \ln(r) + 2\beta^2 E_i(1, k_2 r) \\ - \beta^2 E_i(1, 2k_2 r) + D, \tag{17}$$

with the exponential integral $E_i$ (Jeffreys and Jeffreys 1988) and integration constant $D$. For large $r$, it is required also that $e^{2f(r)} = B_0 r^{(4v^\phi)}$ (Rahaman et al. 2008; Nandi et al. 2009; Chandrasekhar 1983).

By using Eqs. (15) and (16) and the Einasto density profile (Eq. (4)), the Einstein field equations give us the tedious form of the shape function

$$b(r) = \frac{2^{(3-\frac{3}{\alpha})}\pi\rho_0}{\alpha} \exp\left(\frac{2}{\alpha}\right)\left(\frac{(r/r_0)^\alpha r^{-\alpha}}{\alpha}\right)^{-3/\alpha} \\ \times \left[\left(\frac{1}{3(\alpha+3)(2\alpha+3)}\right)\alpha^3 r^3 2^{(3/\alpha - 1 - (\alpha+3)/2\alpha)}\right. \\ \times \left(\frac{(r/r_0)^\alpha r^{-\alpha}}{\alpha}\right)^{3/\alpha}$$
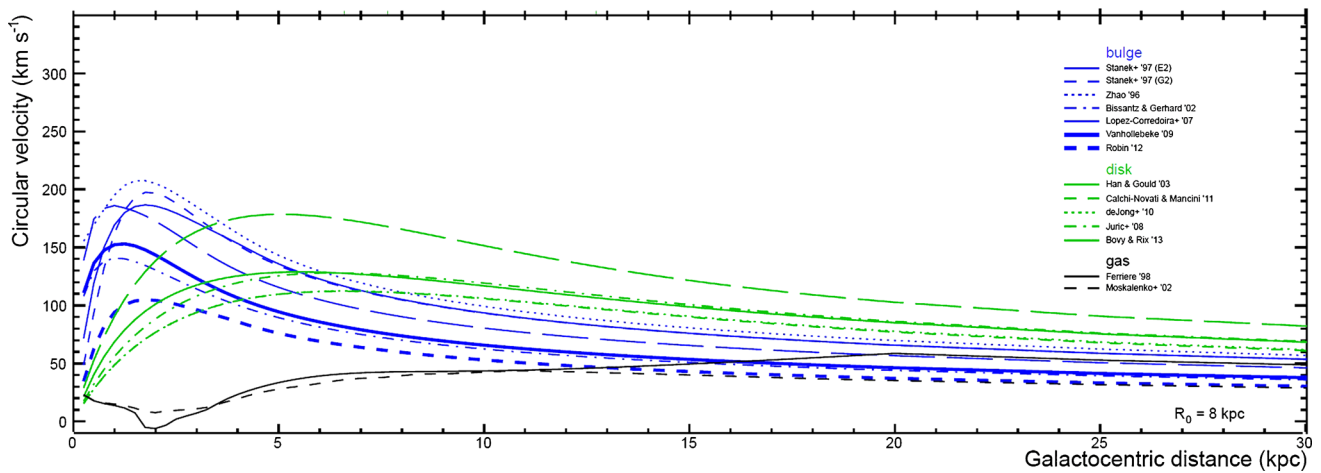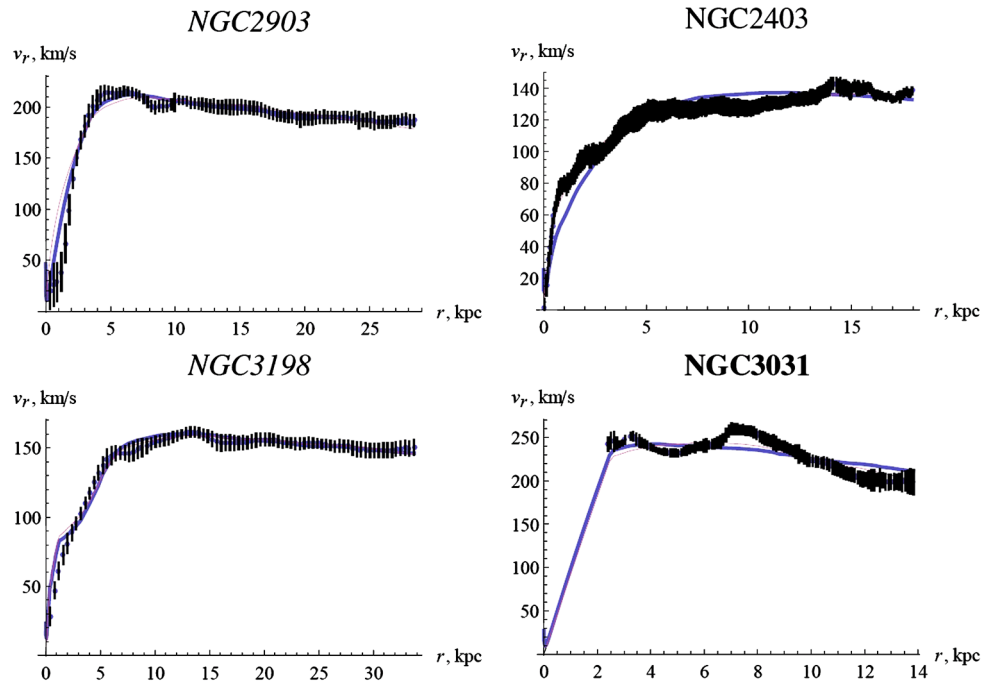
**Fig. 4** Rotational velocity curve for Milkway (the contribution to the rotation curve as predicted from different models for the stellar bulge (*blue*), stellar disk (*green*) and gas (*black*). We assume a distance to the galactic center $r_0 = 8$ kpc (Iocco et al. 2015))

**Fig. 5** Rotational curves $v(r)$ for some galaxies from THINGS survey together with fits. *Blue thick curves* show best fits by DM distributions of semi-degenerate configurations, while *magenta thin curves* show Einasto profile best fits (Siutsou et al. 2015)



$$\times \left(2(r/r_0)^\alpha + \alpha + 3\right)(r/r_0)^{-\alpha}$$

$$\times \left(\frac{(r/r_0)^\alpha}{\alpha}\right)^{-(\alpha+3)/2\alpha}$$

$$\times \exp\left(-\frac{(r/r_0)^\alpha}{\alpha}\right)$$

$$\times WhittakerM\left(3/\alpha - (\alpha+3)/2\alpha,\right.$$

$$\left.(\alpha+3)/2\alpha + 1/2, \frac{2(r/r_0)^\alpha}{\alpha}\right)$$

$$+ \left(\frac{1}{3(2\alpha+3)}\right)\alpha^2 r^3 2^{(3/\alpha-1-(\alpha+3)/2\alpha)}$$

$$\times \left(\frac{(r/r_0)^\alpha r^{-\alpha}}{\alpha}\right)^{3/\alpha}(\alpha+3)(r/r_0)^{-\alpha}$$

$$\times \left(\frac{(r/r_0)^\alpha}{\alpha}\right)^{-(\alpha+3)/2\alpha} \exp\left(-\frac{(r/r_0)^\alpha}{\alpha}\right)$$

$$\times WhittakerM\left(3/\alpha - (\alpha+3)/2\alpha + 1,\right.$$

$$\left.(\alpha+3)/2\alpha + 1/2, \frac{2(r/r_0)^\alpha}{\alpha}\right)\right] + C_1 \qquad (18)$$
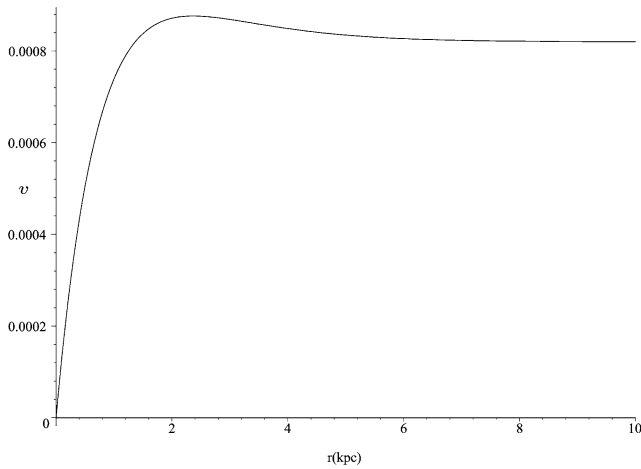
**Fig. 6** Proposed rotational velocity with values of the parameters as $k_1 = k_2 = 1$, $\alpha = 0.0006$ and $\beta = 0.00082$ (Rahaman et al. 2014b)
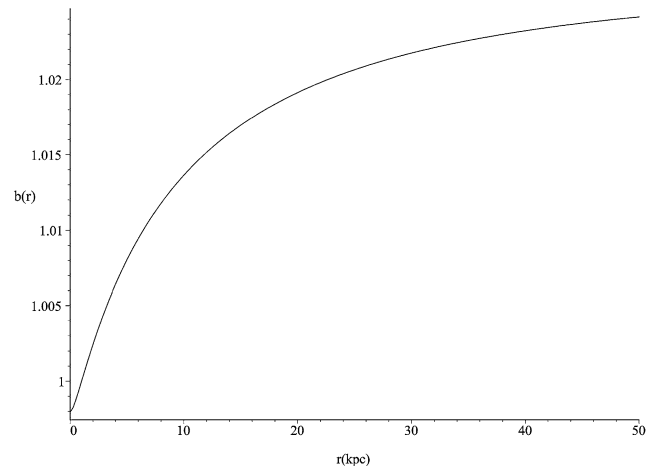


**Fig. 8** The shape function $b$ versus radial coordinate $r$ with the parameters $r_0 = 1$ and $\rho_0 = 0.0001$
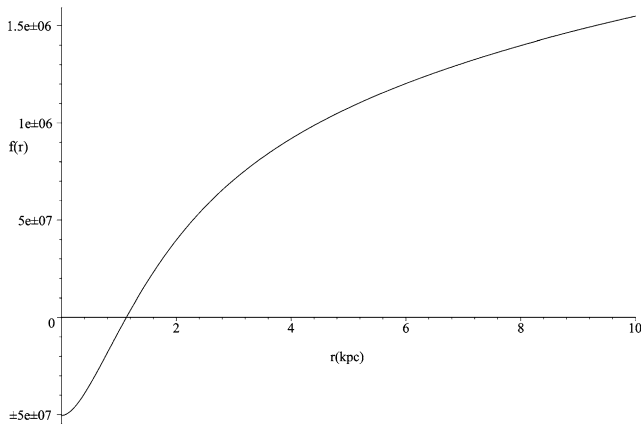


**Fig. 7** $f(r)$ versus $r$ ($k_1 = k_2 = 1$, $\alpha = 0.0006$ and $\beta = 0.00082$ (Rahaman et al. 2014b))
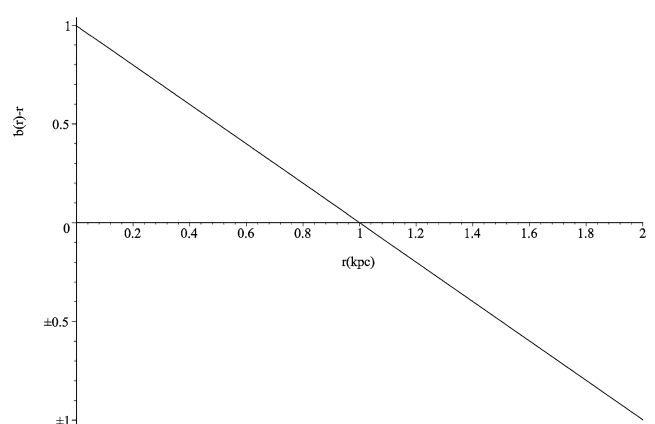


**Fig. 9** The radius of the throat is obtained where $b(r) - r$ cuts $r$ axis or the values $r_0 = 1$ and $\rho_0 = 0.0001$

where the integration constant is chosen as (in order that $b(r_0) = r_0$ is satisfied)

$$
\begin{aligned}
C_1 = {} & \frac{-r_0}{6\alpha^2 + 27\alpha + 27} \Big( A\pi r_0^2 \exp(1/\alpha) 2^{(3\alpha-3)/2\alpha} \\
& \times \alpha^{1+(\alpha+3)/2\alpha} \Big) \\
& \times \Big[ \alpha(5+\alpha) WhittakerM\big(-(\alpha+3)/2\alpha, \\
& \quad (2\alpha+3)/2\alpha, 2/\alpha\big) \\
& + (3+\alpha) WhittakerM\big((\alpha+3)/2\alpha, \\
& \quad (2\alpha+3)/2\alpha, 2/\alpha\big) - 6\alpha - 9 \Big].
\end{aligned}
\tag{19}
$$

Note that in this expression WhittakerM stands for the Whittaker function (Abramowitz and Stegun 1972). The second order differential equation satisfied by $b(r)$ in our present analysis is given by

$$
b'' = \frac{2b'}{r} \left[ 1 - \left( \frac{r}{r_0} \right)^\alpha \right]
\tag{20}
$$

which follows from Eq. (12). The redshift function $f(r)$ versus radial coordinate $r$ is plotted in Fig. 7.

It can be checked that the wormhole throat condition of $b(r_0) = r_0$ is satisfied. It is shown in Figs. 8 and 9. For the Milky Way galaxy, we have $r_0 = 9.11$ kpc and $\rho_0 = 5 \times 10^{-24} (r_0/8.6 \text{ kpc})^{-1}$ g cm$^{-3}$ (Castignani et al. 2012; Maccio et al. 2012; Nesti and Salucci 2013) in order that $r_0$ is greater than the horizon of the supermassive black hole. This is necessary for the wormhole to be traversable. The choice of $r_0$ as throat radius can be justified from the fact that $r_0$ plays the role of the core radius for the galaxy. For this reason we rely on Eq. (4) since for $r > r_0$ there is a turning point for the density distribution. We admit, however, that the exact choice of $r_0$ as the throat radius, unless a better choice is made, is open to criticism. Furthermore, the flare-out condition ($b' < 1$)

$$
b' = 8\pi\rho r^2 = 8\pi r^2 \rho_0 \exp\left[ -\frac{2}{\alpha} \left( \left( \frac{r}{r_0} \right)^\alpha - 1 \right) \right]
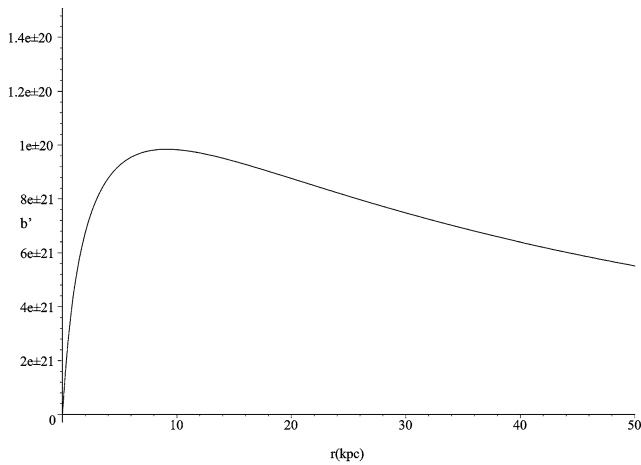\tag{21}
$$

**Fig. 10** $b'$ versus $r$ for Milky Way ($r_0 = 9.11$ kpc and $\rho_0 = 5 \times 10^{-24}(r_0/8.6 \text{ kpc})^{-1} \text{g cm}^{-3}$ (Castignani et al. 2012; Maccio et al. 2012; Nesti and Salucci 2013))
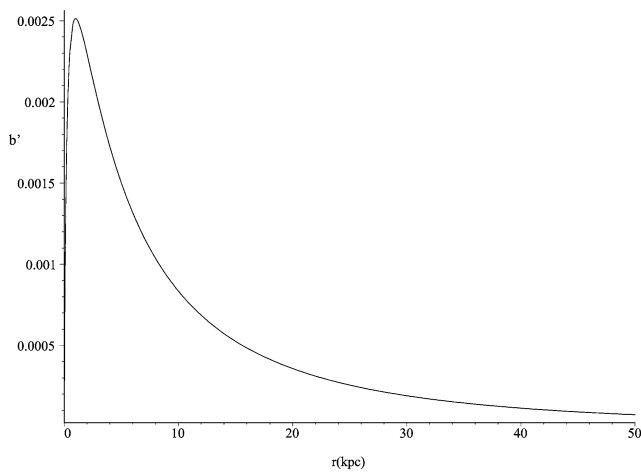


**Fig. 11** $b'$ versus $r$ ($r_0 = 1$ and $\rho_0 = 0.0001$)

is also satisfied for the Milky Way galaxy $b'(r_0) = 0.98 \times 10^{-20} < 1$ (Fig. 10) and also all spherical stellar systems as shown in Fig. 11. In addition, both the star-count and kinematic data of the Milky Way stellar halo are well-represented by an Einasto profile with index $\alpha \approx 0.5$ and effective radius $\approx 20$ kpc, if the dark halo has a flat rotation curve (Figs. 4 and 5) (Evans and Williams 2014).

Finally, for the sake of completeness the radial and lateral pressures are calculated easily from Eqs. (8)–(14) as

$$p_r = \frac{1}{8\pi}\left(\frac{-b}{r^3} + 2\left(1 - \frac{b}{r}\right)\frac{f'}{r}\right), \tag{22}$$

$$p_t = \frac{1}{8\pi}\left\{\left(1 - \frac{b}{r}\right)\left[f'' + f'^2 + \frac{f'}{r} - \left(f' + \frac{1}{r}\right)\left(\frac{b'r - b}{2r(r - b)}\right)\right]\right\} \tag{23}$$
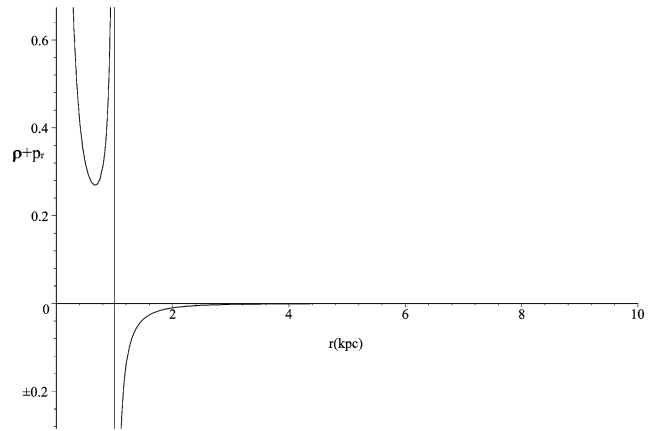


**Fig. 12** Null energy condition ($\rho + p_r < 0$) for the values of parameters $r_0 = 1$ and $\rho_0 = 0.0001$

in which $f(r)$ and $b(r)$ are to be substituted from the solution (Eqs. (17)–(19)).

Note that the null energy condition ($\rho + p_r < 0$) is violated so that the flare-out condition for a wormhole is satisfied according to Fig. 12. Let us note also that those pressures have not been used in the present study but it can be anticipated that for a future stability analysis they will be needed.

## 3 Conclusion

Existence of traversable wormholes is an important problem in physics both at micro and macro scales. There is no doubt that together with black holes wormholes constitute the most interesting objects in our entire universe. On the one hand collision of ultra-energetic particles may create these objects while at the other extreme they form naturally in galactic systems of cosmic dynamics. Once formed, in order to survive traversable wormholes must satisfy certain criteria of stability, otherwise they will decay instantly into more stable objects. Besides stability energy conditions are also of prime importance concerning traversable wormholes. This demands negative energy density which is not available in classical physics although there are rooms for it in the quantum domain. Let us add also that a recent trend is to modify the geometry of throats and obtain thin-shell wormholes (Halilsoy et al. 2014; Ovgun and Sakalli 2015) supported by positive total energy, for this see Mazharimousavi and Halilsoy (2015a, 2015b) and references cited therein. However, the minimum requirement of violationg null-energy condition (NEC) provides that $\rho + p_r < 0$, without specifying the $(-)$ condition for the energy density. As a matter of fact NEC provides us a jumping board into the realm of traversable wormholes. Stability, on the other hand, admittedly and for completely technical reasons remains open in

our present study. This item may be considered as a separate subject in our future analysis.

This work is motivated mainly by Rahaman et al. (2014b), which discusses the possible formation/existence of traversable wormholes in our own galaxy, Milky Way. Their conclusion that traversable wormholes may exist both at the inner and outer parts of our spiral galaxy has been revised by using a different density distribution. Namely, we adapt the Einasto density profile (Einasto 1965; Einasto and Haud 1989) which differs much from the Navarro-Frenk-White (NFW) profile employed in Rahaman et al. (2014b) and Navarro et al. (1996). Our analysis suggests accordingly that at the central region since the NEC is not violated, we do not get any traversable wormholes. This explains also the choice of the throat outside of the central region. Yet at the outer regions, the NEC is violated so that the flare-out condition for traversable wormhole is satisfied and we expect formation of traversable wormholes. This result is not specific to Milky Way alone but is valid for any spiral galaxy once it obeys a mass distribution given by Einosto profile. It is worthwhile therefore to check other mass distributions and see the resulting consequences. In conclusion we wish to comment that the DM lurking in the innermost part of the Milky Way (Iocco et al. 2015), may support the existence of traversable wormholes that contains our solar system as well.

# References

Abramowitz, M., Stegun, I.A. (eds.): Handbook of Mathematical Functions with Formulas, Graphs, and Mathematical Tables, 9th printing Dover, New York (1972)

Bernal, N., Palomares-Ruiz, S.: J. Cosmol. Astropart. Phys., **01**, 006 (2012)

Bozorgnia, N., et al.: J. Cosmol. Astropart. Phys. **1312**, 050 (2013)

Castignani, G., Frusciante, N., Vernieri, D., Salucci, P.: Nat. Sci. **4**, 265 (2012)

Chandrasekhar, S.: Mathematical Theory of Black Holes (Oxford Classic Texts) (1983)

Chan, T.K., et al.: Mon. Not. R. Astron. Soc. **454**(3), 2981–3001 (2015)

Cui, Y.: Mod. Phys. Lett. A **30**(37), 1530028 (2015)

Cline, D.B.: Phys. Scr. **91**(3), 033008 (2016)

Dhar, B.K., Williams, L.L.R.: Mon. Not. R. Astron. Soc. **405**(1), 340 (2010)

Dutton, A.A., Maccio, A.V.: Mon. Not. R. Astron. Soc. **441**(4), 3359 (2014)

Duffy, A.R., et al.: Mon. Not. R. Astron. Soc. **405**(4), 2161–2178 (2010)

Einasto, J.: Tr. Inst. Astrofiz. Alma-Ata **5**, 87 (1965)

Einasto, J., Haud, U.: Galaxy Astron. Astrophys. **223**, 89 (1989)

Einstein, A., Rosen, N.: Phys. Rev. **48**, 73–77 (1935)

Evans, N.W., Williams, A.A.: Mon. Not. R. Astron. Soc. **443**(1) 791 (2014)

Fan, J., Katz, A., Randall, L., Reece, M., Williams, A.A.: Phys. Dark Universe **2**, 139–156 (2013a)

Fan, J., Katz, A., Randall, L., Reece, M.: Phys. Rev. Lett. **110**(21), 211302 (2013b)

Flamm, L.: Phys. Z. **17**, 448 (1916)

Foot, R., Vagnozzi, S.: Phys. Rev. D **91**, 023512 (2015)

Garrett, K., Duda, G., Williams, A.A.: Adv. Astron. **2011**, 968283 (2011)

Gaskins, J.M.: (2016). arXiv:1604.00014

Halilsoy, M., Ovgun, A., Mazharimousavi, S.H.: Eur. Phys. J. **C,74**, 2796 (2014)

Hjorth, J., Williams, L.L.R., Wojtak, R., McLaughlin, M.: (2015). arXiv:1508.02195

Iocco, F., Pato, M., Bertone, G.: Nat. Phys. **11**, 245 (2015)

Jeffreys, H., Jeffreys, B.S.: The exponential and related integrals. In: Methods of Mathematical Physics, 3rd edn., pp. 470–472. Cambridge University Press, Cambridge (1988). §15.09

Kirillov, A.A., Savelova, E.P.: (2015). arXiv:1512.01450

Kuhfittig, P.K.F.: Eur. Phys. J. C **74**, 2818 (2014a)

Kuhfittig, P.K.F.: Found. Phys. **7**, 111–119 (2014b)

Kuhfittig, P.K.F.: Int. J. Mod. Phys. D **24**(03), 1550023 (2015)

Landau, L.D., Lifshitz, E.M.: The Classical Theory of Fields. Pergamon, Oxford (1975)

Lovell, M.R., Frenk, C.S., et al.: Mon. Not. R. Astron. Soc. **439**(1), 300 (2014)

Maccio, A.V., et al.: Astrophys. J. Lett. **744**, L9 (2012)

Mazharimousavi, S.H., Halilsoy, M.: Eur. Phys. J. C **75**(6), 271 (2015a)

Mazharimousavi, S.H., Halilsoy, M.: Eur. Phys. J. C **75**(2), 81 (2015b)

Merritt, D., Graham, A., et al.: Astron. J. **132**, 6 (2006). 2685

Morris, M.S., Thorne, K.S.: Am. J. Phys. **56**, 395 (1988)

Morris, M.S., Thorne, K.S., Yurtsever, U.: Phys. Rev. Lett. **61**, 1446–1449 (1988)

Myrzakulov, R., Sebastiani, L., Vagnozzi, S., Zerbini, S.: (2015). arXiv:1510.02284

Nandi, K.K., Filippov, A.I., Rahaman, F., et al.: Mon. Not. R. Astron. Soc., **399**, 2079 (2009)

Narikawa, T., Yamamoto, K.: J. Cosmol. Astropart. Phys. **05**, 016 (2012)

Navarro, J.F., Frenk, C.S., White, S.D.M.: Astrophys. J. **462**, 563 (1996)

Nesti, F., Salucci, P.: Mon. Not. R. Astron. Soc. **7**, 16 (2013)

Ovgun, A., Sakalli, I.: (2015). arXiv:1507.03949

Pato, M., Iocco, F.: Astrophys. J. **803**, L3 (2015)

Pato, M., Iocco, F., Bertone, G.: J. Cosmol. Astropart. Phys. **1512**(12), 001 (2015)

Ade, P.A.R., et al. (Planck Collaboration): Astron. Astrophys. **571**, A20 (2014)

Poisson, E., Visser, M.: Phys. Rev. D **52**, 7318–7321 (1955)

Rahaman, F., Kalam, M., De Benedictis, A., Usmani, A.A., Ray, S.: Mon. Not. R. Astron. Soc. **27**, 389 (2008)

Rahaman, F., Kuhfittig, P.K.F., Ray, S., Islam, N.: Eur. Phys. J. C **74**, 2750 (2014a)

Rahaman, F., Salucci, P., Kuhfittig, P.K.F., Ray, S., Rahaman, M.: Ann. Phys. **350**, 561–567 (2014b)

Rahaman, F., Shit, G.C., Sen, B., Ray, S.: Astrophys. Space Sci. **361**(1), 37 (2016a)

Rahaman, F., Sen, B., Chakraborty, K., Shit, G.C.: Astrophys. Space Sci. **361**(3), 90 (2016b)

Retana-Montenegro, E., et al.: Astron. Astrophys. **540**, A70 (2012)

Rocha, M., et al.: Mon. Not. R. Astron. Soc. **430**(1), 81–104 (2013)

Salvador-Sole, E., Vinas, J., Manrique, A., Serra, S.: Mon. Not. R. Astron. Soc. **423**(3), 2190 (2012)

Siutsou, I., Arguelles, C.R., Ruffini, R.: Astron. Rep. **59**(7), 656 (2015)

Umetsu, K., Zitrin, A., et al.: (2016). arXiv:1507.04385

Wheeler, J.: Phys. Rev. **97**, 511–536 (1955)

Vera, R.C., Kent, F.W.: Astrophys. J. **159**, 379 (1970)

Vera-Ciro, C.A., Helmi, A., Starkenburg, E., Breddels, M.A.: Mon. Not. R. Astron. Soc. **428**(2), 1696 (2013)

Visser, M.: Phys. Rev. D **39**, 3182–3184 (1989a)

Visser, M.: Nucl. Phys. B **328**, 203–212 (1989b)

Visser, M., Kar, S., Dadhich, N.: Phys. Rev. Lett. **90**, 201102 (2003)

Vogelsberger, M., Zavala, J., Loeb, A.: Mon. Not. R. Astron. Soc. **423**(4), 3740–3752 (2012)

Zwicky, F.: Helv. Phys. Acta **6**, 110–127 (1933)